pp 1833–1843.
doi:10.1017/aer.2021.40

A repairable carbon nanotube web-based electro-thermal heater and damage sensor for aerospace applications

X. Yao
Department of Materials
Henry Royce Institute and National Graphene Institute
University of Manchester
Manchester
UK
and

Advanced Composites Research Group
School of Mechanical and Aerospace Engineering
Queen's University Belfast
Belfast
UK

S.C. Hawkins
Advanced Composites Research Group
School of Mechanical and Aerospace Engineering
Queen's University Belfast
Belfast
UK
and

Department of Materials Science and Engineering
Monash University
Clayton
Australia

B.G. Falzon
b.falzon@qub.ac.uk
Advanced Composites Research Group
School of Mechanical and Aerospace Engineering
Queen's University Belfast
Belfast
UK

Received 26 February 2021; revised 13 April 2021; accepted 21 April 2021.

ABSTRACT

We previously described an efficient, lightweight and flexible electro-thermal system, based on directly drawn carbon nanotube web (CNT web), as part of an icing protection system for carbon fibre reinforced polymer (CFRP) composite aircraft structures. The location of the heating elements on critical lifting surface leading edges or nacelle intake lips makes them particularly susceptible to impact damage, which may leave no visible mark. This makes it desirable to have both a mechanism for identifying the location of damage to the CNT structure (and by inference, potential damage to the underlying CFRP) and a process for restoring the CNT heater to full operation. With the CNT web acting as a sensor, impact damage is identified by an increase in electrical resistance and, particularly, by infrared imaging, which reveals a cold spot or zone depending upon the CNT web layup. Whereas a unidirectional CNT web layup exhibits a large increase in resistance and loss of a full width band of operation, a cross ply quasi-isotropic CNT web arrangement suffers only a small increase in resistance and a loss of function that is highly localised to the damaged area. A novel methodology, based on dispersed CNT in resin, is described for repairing and reconnecting the CNT structure and restoring functionality. A CNT web-based electro-thermal element was applied to the leading edge of a representative carbon-fibre composite wing section to demonstrate the flexibility of this system.

Keywords: carbon nanotube web; electro-thermal system; repairable; sensor; flexible

NOMENCLATURE

AI/DI	anti-icing/de-icing
CF	carbon fibre
CFRP	carbon fibre reinforced polymer
CNT	carbon nanotube
CVD	chemical vapour deposition
GF	glass fibre
GFRP	glass fibre reinforced polymer
ILFT	interlaminar fracture toughness
IR	infrared
LSP	lightning strike protection
R	resistance
SEM	scanning electron microscope
SHM	structural health monitoring
UD	unidirectional
ΔR	change in resistance

1.0 INTRODUCTION

Owing to its superior specific strength and stiffness, carbon fibre reinforced polymer (CFRP) composites are increasingly being used in diverse sectors, such as marine, automotive, sports and, in particular, aerospace, where they comprise around half the weight of the primary

https://doi.org/10.1017/aer.2021.40 Published online by Cambridge University Press

structure of the latest generation wide-body passenger aircraft such as the Boeing 787 and A350 XWB[1]. This revolution in materials and fabrication, together with ever increasing pressure to reduce fuel consumption has provided the impetus for the development of multifunctional structures incorporating such functionality as structural health monitoring (SHM)[2-5], lightning strike protection (LSP)[6-10] and improved ice protection systems[11-18] whilst also delivering enhanced structural performance such as higher interlaminar fracture toughness (ILFT)[19-23].

Directly drawable carbon nanotube web (CNT web) is a uniquely adaptable and useful material composed of highly aligned, small multiwalled CNTs. It is electrically conductive, particularly in the draw direction, extremely light and flexible, and highly compatible with composite materials. We have reported previously on the use of CNT web to address SHM[4] and ILFT[19,20]. We also described the creation of a CNT web-based electrothermal element as part of an AI/DI system for aerospace applications[11-13]. Such an AI/DI element would be located on critical aircraft wing and nacelle lip leading edges, which are also the areas most susceptible to impact. Hence, the AI/DI elements would be the first to suffer impact damage (which may leave no visible mark), necessitating a mechanism to detect damaged areas and to repair them, and this is now reported. The laminate structure of CFRP composite also makes it susceptible to impact damage[24-27]. The mechanism for detection of damage to the AI/DI element also facilitates the localisation of *potential* damage to the underlying CFRP composite, further enhancing the multifunctional value of CNT web. The flexibility of the CNT web-based electrothermal system was demonstrated by applying it to the leading-edge surface of a representative composite wing section provided by Spirit Aerosystems Belfast.

2.0 EXPERIMENTAL SECTION

2.1 Materials and sample preparation

Woven glass fibre (GF)/epoxy prepreg (RE295/SE84LV) and dry woven glass fabric (RE50P), with areal weights of 292 gsm and 47 gsm, respectively, were supplied by Gurit (UK) Ltd. Unidirectional spread tow carbon fibre (UTS50S) thin ply, with an areal weight of 32 gsm[28], was supplied by TeXtreme (Sweden). IN2 epoxy resin and copper foil (0.025 mm thick, annealed, uncoated, 99.8%) were purchased from Easy Composites (UK) and Alfa Aesar (UK), respectively. Highly aligned forests of long, thin, few-wall CNTs were fabricated in-house by chemical vapour deposition (CVD) (Fig. 1a), grown on a silicon wafer with an iron catalyst, yielding an average CNT length of 300 μm (Fig. 1d,e), an average CNT diameter of 10 nm[29,30] and an average wall number of around 7. CNT web was directly drawn from the CNT forests (Fig. 1b-e). The CNT web is highly aligned and anisotropic (orthotropic)[18] with an electrical resistance in the draw direction [0°] only ~4% of that in the transverse direction [90°] (Fig. 1).

Samples, with the number of CNT web layers and their alignment, were arranged in five different layups. Four samples comprised CNT web alone: $[0]_{10}$, $[0]_{20}/[90]_{20}$, $[45]_{20}/[-45]_{20}$ and $[0]_5/[45]_5/[-45]_5/[90]_5$, are denoted A to D. The fifth sample comprised a single layer of unidirectional (UD) thin ply carbon fibre in addition to 20 0° CNT layers, $[0]_{20}/[90*]$ and is denoted E. The thickness of 10 layers of CNT web in resin is ~6 μm, resulting in an overall laminate thickness of 0.60 mm, 0.62 mm, 0.62 mm, 0.61 mm and 0.63 mm for sample A to E. The square heating element comprising the CNT (or CNT/UD thin ply) web stack was sandwiched between two layers of glass fibre reinforced polymer (GFRP) to electrically

https://doi.org/10.1017/aer.2021.40 Published online by Cambridge University Press

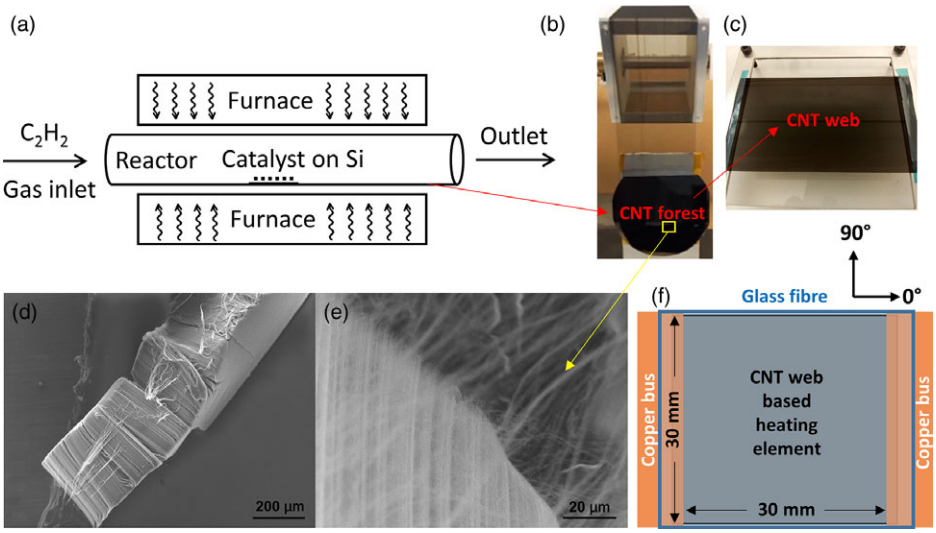

Figure 1. (a) Schematic of CVD. (b) Directly drawn CNT web from CNT forest. (c) CNT web on a mounting frame. SEM images of (d) CNT forest and (e) its drawing. (f) Sample specifications.

isolate it from a putative CFRP structure, and with copper foil buses at two opposite sides in the 90° direction with a final sample size of 30 mm × 30 mm (Fig. 1f). The assembly was prepared using the vacuum bagging technique and cured according to manufacturer (Gurit) specifications for SE84LV.

2.2 Impact damage and repair methods

In order to see the effect of impact damage on, and the repairability of, the CNT web/GFRP electro-thermal system, an in-house constructed dropweight device based on the ASTM D7136 standard, with a 1.266 kg (Fig. 2a), 10 mm diameter hemispherical impactor, and impact energy of 3 J was used. The electrical resistance and thermal performance were measured before and after impact, and damaged samples inspected by SEM. The repair procedure (Fig. 2b-d) entailed preparation of a 1wt% dispersion of the CNT forest in IN2 epoxy resin (resin and slow hardener mixed in the ratio of 100:30) through light roll milling for approximately 1 minute (Fig. 2c) using an in-house built miniature mill. The CNT forests grown by this CVD method are not only able to be drawn into webs, but also very easy to disperse uniformly in epoxy when processed properly. The highly viscous CNT/epoxy mixture was painted onto the impact damaged areas of each sample, which was then placed on an aluminium tool plate. A layer of peel ply and two layers of bleed fabric were applied to the top, and the cure procedure applied according to manufacturer (Easy Composites) specifications for IN2 through vacuum bagging (Fig. 2e).

2.3 Characterization

The resistive heating performance of the composites was investigated, with the voltage and current controlled by an EA Elektro-Automatik PS 3016-20B Digital Bench Power Supply operated at 10 – 12 V (maximum voltage/current: 16 V/20 A). The temperature distribution was monitored by a FLIR SC640 thermal imaging camera (640 × 480 pixels superior resolution, thermal sensitivity of 30 mK, 2°C accuracy), with the samples held horizontally in a still

https://doi.org/10.1017/aer.2021.40 Published online by Cambridge University Press

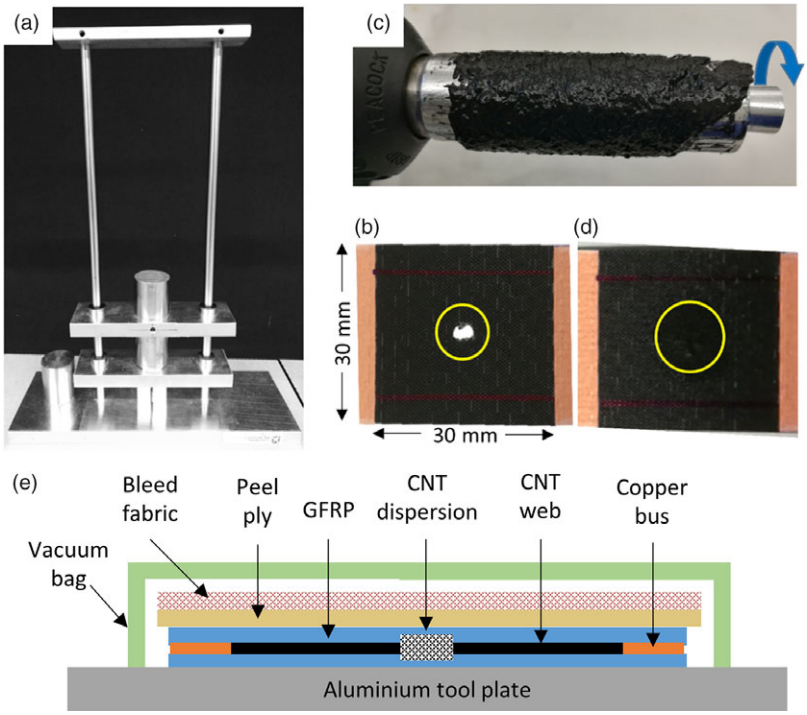

Figure 2. (a) In-house constructed impactors. (b) Sample D after impact. (c) CNTs dispersed in epoxy through roll milling. (d) Dispersed CNT applied to the damaged sample D for repair. (e) Repair through vacuum bagging.

air environment. An Agilent 34450A 5½ Digit Multimeter was employed to measure the resistance of the samples using the 4-wire method. The morphology of CNTs was characterised by a Hitachi FlexSEM1000 Scanning Electron Microscope (SEM).

3.0 RESULTS AND DISCUSSION

3.1 Impact and repair performance of the CNT web-based electrothermal system

Our previous work[11-13] demonstrated the fabrication and performance of CNT web-based electrothermal elements for application in aerospace composites, and how the orthotropic character of the highly aligned CNT web could be designed according to specific requirements[13]. As such systems would be placed on areas susceptible to impact damage, it was evident that a method to detect and repair such damage would be required and is reported here. The methodology depends on the phenomenon of sword-in-sheath breakage commonly observed with small multiwalled CNTs[31] where the outer wall in contact with the matrix fractures while the inner CNT structure partially pulls out before breaking. This creates a fringe of clean CNTs (Fig. 3a,b) along the fracture line that can readily be reconnected. Use of a concentrated dispersion of the same CNT material ensures maximum conformability and connectivity across the break. Whereas the pristine heater uses highly aligned CNT web to

https://doi.org/10.1017/aer.2021.40 Published online by Cambridge University Press

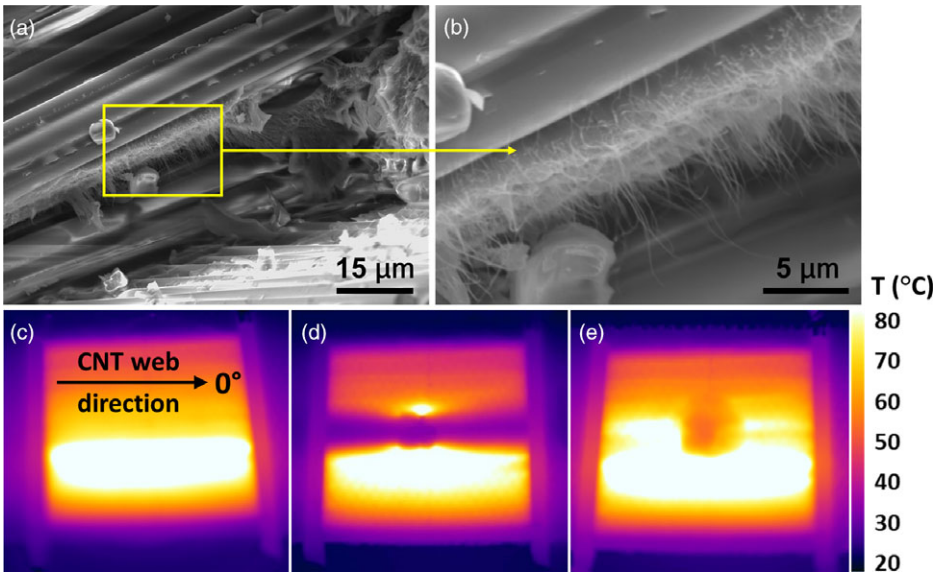

Figure 3. (a) SEM image of fracture edge of Sample A $[0]_{10}$ after impact showing (b) projecting CNT filaments. Thermal performance (c) before and (d) after impact and (e) after repair.

capture the efficiency and flexibility of this material, the repair necessarily uses dispersed or disordered CNT, which is adequate for limited distance conduction that does not degrade the overall heater characteristics. Thus, it should be noted that if a larger damaged region is removed in preparation of a scarf repair, the scale of the CNTs is such that nanoscale CNT protrusions would still be present around the edges. Under such circumstances it is anticipated that a plug patch prefabricated with aligned CNT web could be used with the edges being reconnected using the CNT dispersion.

3.1.1 Unidirectional layup

A simple unidirectional CNT web layup with few web layers (Sample A, $[0]_{10}$), which is most susceptible to inhomogeneities in the web assembly[13], was used to indicate the maximum effect of impact damage (Fig. 3c-e). As the CNT web has low transverse conductivity, heating in the undamaged specimen is slightly uneven (Fig. 3c). However, the impact punched a nearly circular hole through the sample and created an open circuit cold zone across the entire element (Fig. 3d) while the resistance increased by 17.8% (Table 1), which accords with the ratio of the dark (cold) to bright (heated) areas. In addition to being able to draw CNT forests into webs, the CVD CNTs are also very easy to disperse if processed appropriately. After the repair (Fig. 3e), the resistance returned to the value before the impact (Table 1), suggesting that the dispersed CNTs are primarily reconnecting the broken CNT ends protruding from fractures (Fig. 3a,b) rather than forming a bypass or auxiliary heater in their own right.

Once repaired and cured, the broken heating path was almost fully recovered with only a relatively small drop in temperature at and around the impact site of the sample (Fig. 3e). This indicates that the heating characteristic of the mass of dispersed CNTs is not quite as good as that of the CNT web. This may be improved by optimization of the CNT loading or resin cure. A better though slower approach to repairing a sizeable hole might be to prepare a CNT

https://doi.org/10.1017/aer.2021.40 Published online by Cambridge University Press

Table 1
Resistance before and after the impact (3 J) for heaters with different layups

Sample	Heating element – CNT layup	Voltage applied (V)	R-before impact (Ω)	R-after impact (Ω)	ΔR (Ω) ((%))	R-after repair (Ω)	Residual ΔR (Ω) ((%))
A	$[0]_{10}$	12	56.2	66.2	10 (18)	56.2	0 (0)
B	$[0_{20}/90_{20}]$	10	25.6	26.0	0.4 (1.6)	25.9	0.3 (1.2)
C	$[45_{20}/\text{-}45_{20}]$	10	17.5	18.2	0.7 (4)	18.0	0.5 (2.9)
D	$[0_5/45_5/\text{-}45_5/90_5]$	10	53.4	53.9	0.6 (0.9)	53.9	0.5 (0.9)
E	$[0_{20}/90^*_1]$	10	26.3	26.7	0.4 (1.5)	26.7	0.4 (1.5)

∗Note: All the heating elements are made only of CNT web except for sample E where $[90*]_1$ represents 1 layer of CF thin ply, plus 2 layers of GFRP.

web/GFRP patch and join the edges with dispersed CNT in resin. Of particular note is that the heating element can also be used as a sensor by both electrical resistance measurement and especially by infrared (IR) imaging, as it shows the location of damage to the heater structure and, by inference, *potential* damage to the underlying composite.

3.1.2 Cross-ply layups

As a heater with unidirectional CNT web loses a significant area of operation when damaged due to the open circuit and resulting linear unheated area (Fig. 3), it was of importance to determine if a different layup structure could make the heater more resilient to damage (i.e. continue functioning effectively), whilst also providing a better indication of the location and severity of damage. Elements comprising more layers of CNT web and with different layup pattern were prepared (Samples B, C, D). In addition, a CNT heater comprising 20 layers of unidirectional CNT web (0°) plus 1 orthogonal unidirectional thin ply CF layer (i.e. at 90º to the applied electric field) was prepared (Sample E, Table 1). The thin CF ply is approximately 15 μm thick and contributes little to the conductivity or heating function as demonstrated by the resistance, which is very close to that for Sample B ($[0_{20}/90_{20}]$); however, it was anticipated from previous work[12] to provide a useful bridging function for minimal additional weight.

The use of cross-ply layers of CNT (or one CF thin ply) greatly improves the uniformity of heating (Fig. 4) in the CNT web element[18]. Moreover, it dramatically enhances heater resilience, to impact, with the point of impact showing up as a cold spot with only minor to minimal cooling in the zones to either side (Fig. 4) towards the distribution buses. The change in resistance following impact decreased from 10 Ω, or nearly 18% (Sample A) to less than 1 Ω or 4% when cross-ply layups were used (Table 1). After repair there is a small residual increase in resistance of up to 0.5 Ω (2.9%), which possibly reflects the resistance of the CNT dispersion or incomplete reconnection of the broken CNT fringes. Optimisation of the CNT loading and dispersion, and application process are expected to further reduce this disparity.

The linear unheated area seen in the unidirectional sample is almost eliminated by the use of a cross-ply layup such as sample D, which has a quasi-isotropic layup, being marginally more uniform than the other patterns. The actual damage locus is very evident in the cross-ply samples and readily repairable by the method described, with sample D again showing the best uniformity after repair.

https://doi.org/10.1017/aer.2021.40 Published online by Cambridge University Press

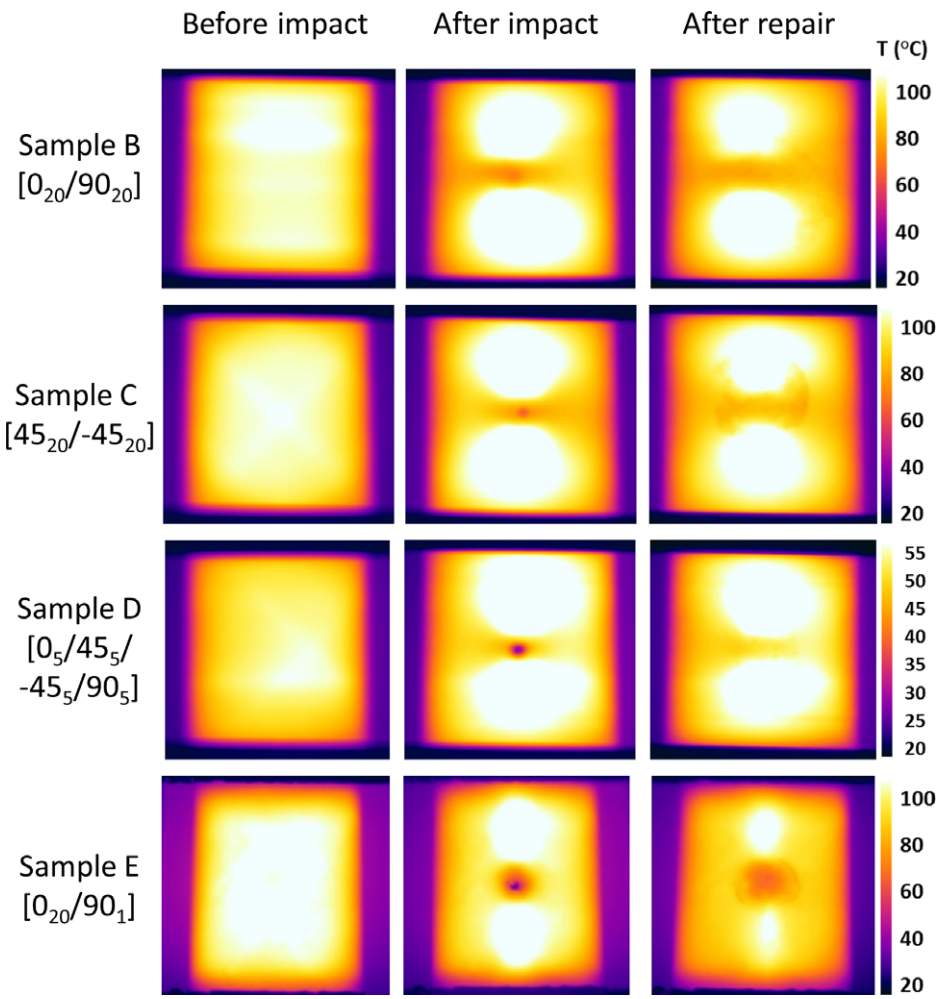

Figure 4. Heating performance of cross-ply samples with different layup before impact, after impact and after repair.

3.2 Flexibility of the CNT web-based electro-thermal system

In addition to its repairability and sensing function, the flexibility of the CNT web-based electro-thermal system was investigated with the CNT web layers ($[0]_{15}$) embedded between two layers of dry woven glass fabric (RE50P). The CNT/GFRP assembly was fabricated by vacuum-assisted resin infusion using IN2 resin. After curing (Fig. 5a), the device was cut into the shape of a model wing leading edge section (Fig. 5b) and applied to its surface (Fig. 5c). The device was fabricated with unidirectional (0°) CNT web, so the orthogonally oriented anisotropy of this structure results in the resistance increasing from 178 Ω to 462 Ω when cut from a rectangular (Fig. 5a) to a chevron shape (Fig. 5b) to conform to the leading edge profile. At the maximum voltage (16 V) applied, the IR image (Fig. 5d) shows the highly conformal device as well as the effect of using the unidirectional CNT web, with the warmest zone corresponding to the most direct conduction path, as discussed in an earlier paper[13].

https://doi.org/10.1017/aer.2021.40 Published online by Cambridge University Press

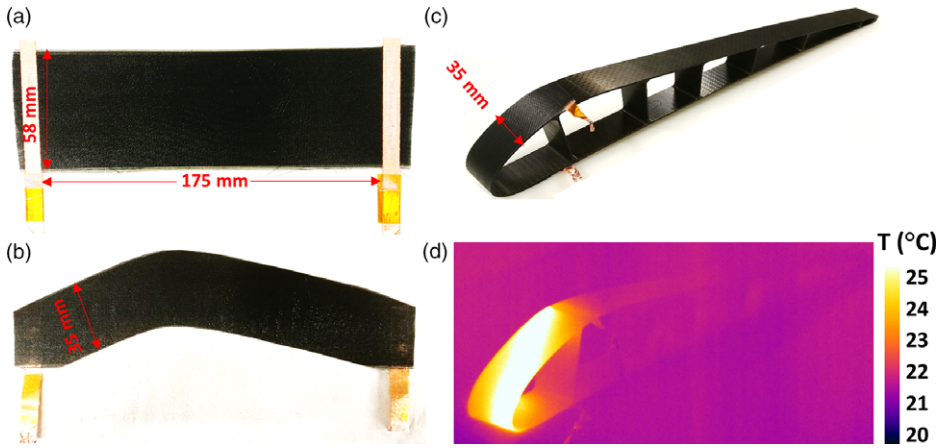

Figure 5. CNT web/glass fabric composite heater (a) original sample, (b) after being cut into a conformal shape, then (c) applied onto the aircraft wing section and (d) heating performance viewed by IR camera.

4.0 CONCLUSIONS

Directly drawn CNT web has been demonstrated to produce a flexible, efficient, lightweight electro-thermal heating system. The CNT web is highly anisotropic with current flow primarily in the draw direction, so the layup pattern has a significant effect on the heating efficiency, thermal distribution and impact tolerance of the heater but also allowing for the design of layup patterns to achieve a predictable heat distribution. The unidirectional layup, where there is very little transverse conductivity and hence pathway for current in the event of a breakage, after impact, exhibited near-complete open circuit and heating failure in line with the damage. However, a method was developed so that this could be easily and quickly repaired with dispersed CNTs. Furthermore, through designing the layup, the heating element can be made much more resilient to damage with minimal change in resistance and performance as a result of impact damage whilst retaining the capacity to exhibit damage by IR photography. Repair is equally simple for such damage. In addition, the flexibility of the CNT web-based electro-thermal system was demonstrated through fabricating a CNT/GF/epoxy composite and applying to the surface of the leading edge of a representative composite wing section.

ACKNOWLEDGEMENTS

The authors would like to acknowledge the financial support received from the European Union's 7th Framework Programme for Research under the Marie Curie Career Integration grant agreement No. 630756. We also acknowledge EP/N007190/1, the UK Engineering and Physical Sciences Research Council (EPRSC) grant.

REFERENCES

1. MCCONNELL V.P. Past is prologue for composite repair. *Reinf Plast,* 2011, **55**, (6), pp 17–21.
2. DIAMANTI K. and SOUTIS C. Structural health monitoring techniques for aircraft composite structures. *Prog Aerosp Sci,* 2010, **46**, (8), pp 342–352.

https://doi.org/10.1017/aer.2021.40 Published online by Cambridge University Press

3. GUEMES A., FERNANDEZ L.A., POZO A.R. and SIERRA P.J. Structural health monitoring for advanced composite structures: a review. *J Compos Sci,* 2020, **4**, (13), pp 1–15.
4. KUMAR S., FALZON B.G. and HAWKINS S.C. Ultrasensitive embedded sensor for composite joints based on a highly aligned carbon nanotube web. *Carbon,* 2019, **149**, pp 380–389.
5. GAO L., CHOU T.W., THOSTENSON E.T., ZHANG Z. and COULAUD M. In situ sensing of impact damage in epoxy/glass fiber composites using percolating carbon nanotube networks. *Carbon,* 2011, **49**, (10), pp 3382–3385.
6. ZHANG B., SOLTANI S.A., LE L.N. and ASMATULU R. Fabrication and assessment of a thin flexible surface coating made of pristine graphene for lightning strike protection. *Mater Sci Eng B,* 2017, **216**, pp 31–40.
7. YAMASHITA S., HIRANO Y., SONEHARA T., TAKAHASHI J., KAWABE K. and MURAKAMI T. Residual mechanical properties of carbon fibre reinforced thermoplastics with thin-ply prepreg after simulated lightning strike. *Compos Part A,* 2017, **101**, pp 185–194.
8. WANG B., DUAN Y., XIN Z., YAO X., ABLIZ D. and ZIEGMANN G. Fabrication of an enriched graphene surface protection of carbon fiber/epoxy composites for lightning strike via a percolating-assisted resin film infusion method. *Compos Sci Technol,* 2018, **158**, pp 51–60.
9. GUO Y., DONG Q., CHEN J., YAO X., YI X. and JIA Y. Comparison between temperature and pyrolysis dependent models to evaluate the lightning strike damage of carbon fiber composite laminates. *Compos Part A,* 2017, **97**, pp 10–18.
10. GUO Y., XU Y., WANG Q., DONG Q., YI X. and JIA Y. Eliminating lightning strike damage to carbon fiber composite structures in Zone 2 of aircraft by Ni-coated carbon fiber nonwoven veils. *Compos Sci Technol,* 2019, **169**, pp 95–102.
11. YAO X., FALZON B.G., HAWKINS S.C. and TSANTZALIS S. Aligned carbon nanotube webs embedded in a composite laminate: A route towards a highly tunable electro-thermal system. *Carbon,* 2018, **129**, pp 486–494.
12. YAO X., HAWKINS S.C. and FALZON B.G. An Advanced Anti-icing/De-icing system utilizing highly aligned carbon nanotube webs. *Carbon,* 2018, **136**, pp 130–138.
13. YAO X., FALZON B.G. and HAWKINS S.C. Orthotropic electro-thermal behaviour of highly-aligned carbon nanotube web based composites. *Compos Sci Technol,* 2019, **170**, pp 157–164.
14. TARFAOUI M., MOUMEN A.E., BOEHLE M., SHAH O. and LAFDI K. Self-heating and deicing epoxy/glass fiber based carbon nanotubes buckypaper composite. *J Mater Sci,* 2019, **54**, (2), pp 1351–1362.
15. IBRAHIM Y., KEMPERS R. and AMIRFAZLI A. 3D printed electro-thermal anti- or de-icing system for composite panels. *Cold Reg Sci Technol,* 2019, **166**, pp 102844.
16. ZANGROSSI F., XU F., WARRIOR N., KARAPAPPAS P. and HOU X. Electro-thermal and mechanical performance of multi-wall carbon nanotubes buckypapers embedded in fibre reinforced polymer composites for ice protection applications. *J Compos Mater,* 2020, **54**, (23), pp 3457–3469.
17. REDONDO O., PROLONGO S.G., CAMPO M., SBARUFATTI C. and GIGLIO M. Anti-icing and de-icing coatings based Joule's heating of graphene nanoplatelets. *Compos Sci Technol,* 2018, **164**, pp 65–73.
18. ZHAO Z., CHEN H., LIU X., LIU H. and ZHANG D. Development of high-efficient synthetic electric heating coating for anti-icing/de-icing. *Surf Coatings Technol,* 2018, **349**, pp 340–346.
19. NISTAL A., FALZON B.G., HAWKINS S.C., CHITWAN R., GARCIA D.C. and RUBIO F. Enhancing the fracture toughness of hierarchical composites through amino–functionalised carbon nanotube webs. *Compos Part B,* 2019, **165**, pp 537–544.
20. LEONARDO S.D., NISTAL A., CATALANOTTI G., HAWKINS S.C. and FALZON B.G. Mode I interlaminar fracture toughness of thin-ply laminates with CNT webs at the crack interface. *Compos Struct,* 2019, **225**, pp 111178.
21. WICKS S.S., WANG W., WILLIAMS M.R. and WARDLE B.L. Multi-scale interlaminar fracture mechanisms in woven composite laminates reinforced with aligned carbon nanotubes. *Compos Sci Technol,* 2014, **100**, pp 128–135.
22. KALFON C.E., KOPP R., FURTADO C., NI X., ARTEIRO A., BORSTNAR G., *et al.*et al. Synergetic effects of thin plies and aligned carbon nanotube interlaminar reinforcement in composite laminates. *Compos Sci Technol,* 2018, **166**, pp 160–168.
23. OU Y., GONZALEZ C. and VILATELA J.J. Interlaminar toughening in structural carbon fiber/epoxy composites interleaved with carbon nanotube veils. *Compos Part A,* 2019, **124**, pp 105477.

https://doi.org/10.1017/aer.2021.40 Published online by Cambridge University Press

24. DONADON M.V., IANNUCCI L., FALZON B.G., HODGKINSON J.M. and ALMEIDA S.F.M. A progressive failure model for composite laminates subjected to low velocity impact damage. *Comput Struct,* 2008, **86**, pp 1232–1252.
25. FALZON B.G., ROBINSON P., FRENZ S. and GILBERT B. Development and evaluation of a novel integrated anti-icing/de-icing technology for carbon fibre composite aerostructures using an electro-conductive textile. *Compos Part A,* 2015, **68**, pp 323–335.
26. HEIMBS S., HELLER S., MIDDENDORF P., HAHNEL F. and WEIBE J. Low velocity impact on CFRP plates with compressive preload: Test and modelling. *Int J Impact Eng,* 2009, **36**, pp 1182–1193.
27. FAGGIANI A. and FALZON B.G. Predicting low-velocity impact damage on a stiffened composite panel. *Compos Part A,* 2010, **41**, (6), pp 737–749.
28. RUSSELLO M., DIAMANTI E.K., CATALANOTTI G., OHLSSON F., HAWKINS S.C. and FALZON B.G. Enhancing the electrical conductivity of carbon fibre thin-ply laminates with directly grown aligned carbon nanotubes. *Compos Struct,* 2018, **206**, pp 272–278.
29. ATKINSON K.R., HAWKINS S.C., HUYNH C., SKOURTIS C., DAI J., ZHANG M., *et al.*et al. Multifunctional carbon nanotube yarns and transparent sheets: Fabrication, properties, and applications. *Physica B,* 2007, **394**, pp 339–343.
30. HUYNH C.P. and HAWKINS S.C. Understanding the synthesis of directly spinnable carbon nanotube forests. *Carbon,* 2010, **48**, (4), pp 1105–1115.
31. YU M.F., LOURIE O., DYER M.J., MOLONI K., KELLY T.F. and RUOFF R.S. Strength and breaking mechanism of multiwalled carbon nanotubes under tensile load. *Science,* 2000, **287**, (5453), pp 637–640.

https://doi.org/10.1017/aer.2021.40 Published online by Cambridge University Press